



**HAL**  
open science

## Chemical composition of the snowpack during the OASIS spring campaign 2009 at Barrow, Alaska

Hans-Werner Jacobi, D. Voisin, J. Jaffrezo, J. Cozic, T. Douglas

► **To cite this version:**

Hans-Werner Jacobi, D. Voisin, J. Jaffrezo, J. Cozic, T. Douglas. Chemical composition of the snowpack during the OASIS spring campaign 2009 at Barrow, Alaska. *Journal of Geophysical Research: Atmospheres*, 2012, 117 (D14), 10.1029/2011JD016654 . hal-04702982

**HAL Id: hal-04702982**

**<https://hal.science/hal-04702982v1>**

Submitted on 23 Sep 2024

**HAL** is a multi-disciplinary open access archive for the deposit and dissemination of scientific research documents, whether they are published or not. The documents may come from teaching and research institutions in France or abroad, or from public or private research centers.

L'archive ouverte pluridisciplinaire **HAL**, est destinée au dépôt et à la diffusion de documents scientifiques de niveau recherche, publiés ou non, émanant des établissements d'enseignement et de recherche français ou étrangers, des laboratoires publics ou privés.

Copyright

## Chemical composition of the snowpack during the OASIS spring campaign 2009 at Barrow, Alaska

H. W. Jacobi,<sup>1</sup> D. Voisin,<sup>1</sup> J. L. Jaffrezo,<sup>1</sup> J. Cozic,<sup>1</sup> and T. A. Douglas<sup>2</sup>

Received 30 July 2011; revised 18 January 2012; accepted 23 January 2012; published 14 March 2012.

[1] The chemical composition of the seasonal snowpack was determined close to Barrow, an Arctic coastal location in northern Alaska. One hundred and twelve samples of different snow types including fresh snow, surface hoar, diamond dust, blowing snow, rounded snow grains, and depth hoar were collected and analyzed for major sea salt components, bromide, and nitrate. Sodium, chloride, sulfate, and potassium are mainly introduced into the snowpack by the deposition of sea salt, while magnesium and calcium result from a combination of sea salt and dust. Sulfate was strongly depleted in most samples compared to other sea salt components. This is attributed to the precipitation of mirabilite in newly formed sea ice and frost flowers that leads to an efficient fractionation of sulfate. Uptake of volatile but soluble species from the gas phase also contributed to the observed chloride, sulfate, and nitrate in the snow. However, for chloride and sulfate the input from the marine sources was overwhelming and the uptake from the gas phase was only visible in the samples with low concentrations like fresh snow, diamond dust, and surface hoar. Nitrate concentrations in the snowpack were less variable and for aged snow nitrate was related to the specific surface area of the snow indicating the adsorption of nitric acid can be an important nitrate source in the aged snow. Bromide was also introduced into the snowpack from marine sources, but due to its high reactivity it was partly transferred back to the atmosphere in the form of reactive species. The result of these processes was evident in bromide concentrations, which were both enriched and depleted at the snowpack surface while deeper layers were mostly depleted. Blowing snow also exhibited a depleted bromide composition. For all compounds except nitrate, many depth hoar samples exhibited the greatest concentrations, probably as a result of higher input earlier in the season as well as increases due to the sublimation of water during the metamorphism of the snow.

**Citation:** Jacobi, H. W., D. Voisin, J. L. Jaffrezo, J. Cozic, and T. A. Douglas (2012), Chemical composition of the snowpack during the OASIS spring campaign 2009 at Barrow, Alaska, *J. Geophys. Res.*, *117*, D00R13, doi:10.1029/2011JD016654.

### 1. Introduction

[2] Photochemical processes in snow lead to the formation of reactive compounds that can be released to the atmosphere and impact the chemical composition of the atmospheric boundary layer [Grannas *et al.*, 2007]. At an Arctic coastal location like Barrow, Alaska, these processes play a role in the activation of halogen compounds and the formation of nitrogen oxides. The precursors of the reactive species are chloride, bromide, and nitrate [Simpson *et al.*, 2007; Grannas *et al.*, 2007]. To constrain formation processes and production rates of the reactive species a comprehensive knowledge of the distribution of precursors in the snowpack is needed. Moreover, a better understanding of the processes that

control the input of the different precursors can help to better describe the chemical composition of the snowpack and how chemical processes may change during the winter season.

[3] Photochemical transformation processes in the snow depend not only on concentrations of stable precursors but also on the overall composition of the snow. Impurities in the snow are at least partly excluded from the solid ice crystal and contribute to the formation of a liquid fraction in the form of concentrated brine at temperatures well below the melting point of ice [e.g., Cho *et al.*, 2002]. Complex photochemical transformations can occur in this phase. The volume of the liquid fraction available depends on the snow temperature and on the amount of impurities in the snow [e.g., Wettlaufer, 1999; Cho *et al.*, 2002; Kuo *et al.*, 2011]. As a consequence, a full chemical budget of the snowpack is needed to constrain and model chemical processes that occur in the snowpack. At coastal locations like Barrow the chemical budget of the snow is usually dominated by the presence of sea salt and its components. Therefore, sea salt components can be used to estimate the total budget of impurities in the snowpack.

<sup>1</sup>Laboratoire de Glaciologie et Géophysique de l'Environnement, UMR 5183, CNRS/Université Joseph Fourier – Grenoble 1, Grenoble, France.

<sup>2</sup>Environmental Sciences, U.S. Army Cold Regions Research and Engineering Laboratory, Fort Wainwright, Alaska, USA.

[4] Although dominated by the input from sea salt generated by marine sources, the chemical composition of the snowpack at Arctic coastal locations shows a significant variability. This is related to the fact that at this high latitude different marine sources for sea salt aerosols like open water in polynyas and leads and different types of sea ice exist. For example, the formation of new sea ice and frost flowers can lead to the modification of the composition of mobilized sea salt aerosols. If temperatures in the sea ice drop below certain thresholds, compounds like mirabilite can precipitate leading to a reduction of sulfate [Wagenbach *et al.*, 1998; Alvarez-Aviles *et al.*, 2008]. The chemistry of the snowpack in the Arctic is further modified by multiple processes like deposition of dust or aerosols from lower latitudes that contribute to the so-called Arctic Haze [Barrie and Hoff, 1985; Snyder-Conn *et al.*, 1997; Garbarino *et al.*, 2002; Douglas and Sturm, 2004]. Many cryospheric processes related to sea ice and snow are currently undergoing rapid changes in the Arctic [e.g., Lemke *et al.*, 2007]. Therefore, a better comprehension of the chemical composition of the Arctic snowpack and how it is modified in a changing environment is needed.

[5] Previous chemical analysis of snow samples in the geographical region between Barrow and the Brooks Range approximately 300 km south have been performed by Douglas and Sturm [2004], Simpson *et al.* [2005], and Douglas *et al.* [2008]. Simpson *et al.* [2005] collected surface snow samples without distinguishing the snow type and determined sodium, chloride, and bromide. Mercury was analyzed in the samples collected by Douglas *et al.* [2008] and concentrations were grouped according to different snow types. Further analysis of the chemical composition of snow was performed by Toom-Sauntry and Barrie [2002] to determine major ions (including bromide) and organic ions. Between 1990 and 1994 they collected fresh snow close to Alert on the Canadian Arctic Ocean coast under low wind conditions to avoid mixing with blowing snow. Their results showed that sulfate and calcium were the dominant ions at this location. Furthermore, the ionic balance showed a seasonal cycle with acids (mainly sulfates and nitrates) dominating between March and May. Chloride and bromide were always enriched due to uptake from the gas phase. However, the enrichment of bromide became more important in the snowpack after sunrise at springtime.

[6] Here we report results from the analysis of more than 110 snow samples collected in springtime 2009 during the international multidisciplinary Ocean-Atmosphere-Sea Ice-Snowpack (OASIS) campaign in Barrow, Alaska. All samples were collected onshore representing six morphological snow grain shape classes: precipitation particle types, surface hoar, decomposing and fragmented precipitation particles, rounded grains, depth hoar, and melt forms. Analyzed species included major and minor sea salt components (chloride, sulfate, sodium, potassium, magnesium, calcium, bromide) and nitrate. The results were used to determine the average composition of the snowpack and to identify the major sources for the different species in the snow. The results were further analyzed to quantify important processes in the snow contributing to a better comprehension of how the chemical composition of the seasonal snowpack is controlled by the input from different marine and continental sources and subsequent physical and chemical processes

occurring in the snowpack and the atmosphere. This includes the major precursors for photochemical processes like chloride, bromide, and nitrate. The data set was also used to investigate the impact of atmospheric and snow photochemical processes on the concentrations of major and minor ions in the snow.

## 2. Methods

### 2.1. Snow Sampling

[7] We collected snow near Barrow, Alaska near the Arctic Coastal Plain (ACP) between 4 March and 11 April 2009 during the OASIS spring campaign 2009. All samples were collected and stored in borosilicate glass containers. Most of the samples were collected on top of the tundra in an area southeast of the Barrow Arctic Research Center (BARC, 71.3°N, 156.7°W) located approximately 1.5 km south of the Chukchi Sea Coast. This area is underlain by continuous permafrost and the surface topography is of an extremely low gradient and contains numerous shallow lakes. Since the snowpack exhibits different properties on the tundra versus the lakes of the ACP [Sturm and Liston, 2003] we did not collect samples on lakes. Additionally, the lakes may not contain the early season snow that falls prior to ice formation so the full winter record cannot be collected on lakes. All samples were collected at a distance of at least 100 m of the BARC building. On 27 March six snow samples were collected approximately 15 km inland (71.21°N, 156.47°W) to test if emissions caused by local anthropogenic activities contributed to the observed snow composition. For all investigated compounds no differences were found for the BARC and inland tundra locations (see auxiliary material Data Set S1).<sup>1</sup> Therefore, the results of all collected samples were used for further analysis.

[8] At both locations, the snowpack was characterized by heterogeneous physical properties and varying snow types [Domine *et al.*, 2012]. Typically, it consists of 4 or more layers with an average snow height on the order of 40 cm and snow densities between 0.16 and 0.38 g cm<sup>-3</sup>. A large fraction (more than 50%) of the total snowpack consisted of depth hoar normally located at the bottom of the snowpack, but sometimes also encountered at higher layers. The properties were comparable to the ACP snowpack on land as observed in previous years [Sturm and Liston, 2003; Douglas *et al.*, 2008]. According to the recording of the snow height at the airport of Barrow, a large fraction of the snow had already accumulated by the first week of October 2008. Further accumulation occurred throughout the winter season with the most significant accumulation events in the second half of January 2009 and mid-February.

[9] The depth, thickness, and snow type were recorded for each snow sample (See auxiliary material Data Set S1). Snow samples were grouped into eight different categories: fresh snow (FS), diamond dust/surface hoar (DD/SH), blowing snow (FBS), blown snow (BS), wind-packed snow (WP), wind-packed snow at the surface (WPS), snow with ice layers (I), and depth hoar (DH). These categories correspond to the main morphological grain shape class precipitation

<sup>1</sup>Auxiliary material data sets are available at <ftp://ftp.agu.org/apend/jd/2011/jd016654>. Other auxiliary material files are in the HTML. doi:10.1029/2011JD016654.

**Table 1.** Summary of the Sampled Snow Types, Their Characteristics, Sampling Technique, Classification According to the International Classification for Seasonal Snow, and the Processes Impacting the Chemical Composition<sup>a</sup>

Snow Type	Characteristics	Sampling	Classification	Chemical Composition
Fresh snow (FS)	Crystals formed in clouds	Collected on trays or on top of a re-frozen layer	Precipitating particles (Accumulation)	Composition of ice nucleating particles, uptake from gas phase, scavenging, riming
Diamond dust/surface hoar (DD/SH)	Crystals formed from water vapor by rapid kinetic growth in the atmosphere or at the snow surface	Collected on top of a re-frozen layer	Precipitating particles, surface hoar (Accumulation)	Composition of ice nucleating particles, uptake from gas phase
Blowing snow (FBS)	Older snow grains mobilized by creep, saltation, and suspension	Bottles filled automatic by mobilized snow	Decomposing and fragmented precipitation particles (Accumulation)	Composition of mobilized snow, incorporation of aerosols
Blown snow (BS)	Recently deposited snow	Snow drifts	Decomposing and fragmented precipitation particles (Deposited snow)	Composition of accumulated snow, deposition, post-depositional loss
Wind-packed snow (WP)	Rounded and well sintered grains	Snow pit	Rounded grains (Deposited snow)	Same as for blown snow
Wind-packed snow at the surface (WPS)	Rounded and well sintered grains	Snow pit	Rounded grains (Deposited snow)	Same as for blown snow
Snow with ice layers (I)	Layers with ice	Snow pit	Melt forms (Deposited snow)	Same as for blown snow
Depth hoar (DH)	Hexagonal cups as a result of efficient snow metamorphism	Snow pit	Depth hoar (Deposited snow)	Same as for blown snow

<sup>a</sup>See Fierz *et al.* [2009].

particle types (FS, DD), surface hoar (SH), decomposing and fragmented precipitation particles (FBS, BS), rounded grains (WP, WPS), depth hoar (DH), and melt forms (I) according to the International Classification for Seasonal Snow [Fierz *et al.*, 2009]. The different snow types and their characteristics are briefly summarized in Table 1.

[10] Four FS samples were collected from the snow surface after precipitation events on 1, 4, and 5 April. Under specific meteorological conditions (low temperatures, high saturation in water vapor, low wind speeds), surface hoar and diamond dust grow directly from the vapor phase [e.g., Feick *et al.*, 2007; Douglas *et al.*, 2008]. On 18 and 19 March meteorological conditions were favorable for the formation of SH on the snowpack surface and deposition of DD from the atmosphere. These samples were collected on top of a refrozen layer on the snowpack surface. They contained an estimated fraction of 40% SH. The physical properties and chemical composition are discussed in detail by Domine *et al.* [2011]. To collect FBS sample bottles were placed downwind of a snow ridge with the rim of the bottle exposed above the snow surface by less than 5 cm. The bottles were filled after several minutes. BS samples were collected in snow drifts. WPS and DH were sampled throughout the campaign at different depths in the snowpack. WPS samples were exposed at the snow surface before sampling and showed clear signs of wind erosion. Seven snow samples including ice layers were collected on 17 and 18 March. The ascribed categories indicate the dominant snow type for each sample. A total of 112 samples were collected. The samples were stored in a cold room at the BARC facility at  $-30^{\circ}\text{C}$  until shipping to Grenoble, France in insulated boxes. The samples were stored frozen until analysis.

## 2.2. Analysis

[11] Concentrations of sodium ( $\text{Na}^+$ ), potassium ( $\text{K}^+$ ), magnesium ( $\text{Mg}^{2+}$ ), calcium ( $\text{Ca}^{2+}$ ), chloride ( $\text{Cl}^-$ ), sulfate ( $\text{SO}_4^{2-}$ ), nitrate ( $\text{NO}_3^-$ ), and bromide ( $\text{Br}^-$ ) were determined by ion chromatography. Cations were analyzed with a Dionex DX100 (Sunnyvale, California) on a CS12 column with suppressed conductivity detection. Anions were analyzed with a Dionex DX500 on an AS11 column with suppressed conductivity detection. Details on the analytical methods are described by Jaffrezo *et al.* [1998] and Ricard *et al.* [2002]. Samples were filtered using  $0.22\ \mu\text{m}$  Acrodisc filters before analysis. The detection limit is typically below  $1\ \mu\text{g L}^{-1}$  for all measured compounds. The analytical precision obtained from the standard deviation of multiple analyses of the same sample or standard is around 10% for  $\text{Br}^-$  and below 5% for the remaining ions. A limited number of samples were collected as triplicates and they exhibited a variability of 8–15% which is slightly higher than the analytical uncertainty.

## 3. Results

[12] All measured concentrations are summarized in auxiliary material Data Set S1. The concentrations of the single samples were first analyzed to investigate the temporal development of the composition of the snowpack. Since the main objective of the study was to determine the exchange of trace compounds between snow and atmosphere the top snow layers were sampled more frequently than the deeper or bottom layers of the snowpack. No consistent overall

**Table 2.** Summarizing Statistics of Measured Snow Concentrations (in  $\mu\text{g L}^{-1}$ ) Grouped According to Snow Types<sup>a</sup>

Snow Type	Summary Statistics	Cl <sup>-</sup>	NO <sub>3</sub> <sup>-</sup>	SO <sub>4</sub> <sup>2-</sup>	Na <sup>+</sup>	K <sup>+</sup>	Mg <sup>2+</sup>	Ca <sup>2+</sup>	Br <sup>-</sup>
FS (N = 4)	Average	1712	252	204	734	25	141	117	29
	St.dev.	1020	19	46	559	15	113	66	10
	Median	1723	256	205	750	24	119	112	26
	Minimum	705	227	159	217	12	44	58	21
	Maximum	2696	268	248	1221	42	283	185	42
DD/SH (N = 7)	Average	985	141	257	367	25	79	155	48
	St.dev.	439	19	68	276	14	88	106	11
	Median	837	141	257	329	25	58	113	40
	Minimum	542	112	173	110	5	20	57	37
	Maximum	1849	165	350	954	51	274	367	64
FBS (N = 15)	Average	14756	229	733	7903	307	1449	630	59
	St.dev.	14583	43	544	7821	312	1241	481	76
	Median	8506	213	462	4559	171	1098	576	20
	Minimum	2593	176	249	1485	41	266	155	11
	Maximum	42171	339	1750	23337	917	3778	1492	244
BS (N = 32)	Average	11704	277	623	6442	248	1374	664	47
	St.dev.	7982	67	325	4556	180	891	354	46
	Median	7995	284	470	4461	175	1102	665	22
	Minimum	2454	130	300	1231	38	245	170	9
	Maximum	29838	388	1256	17271	681	3527	1444	190
WP (N = 22)	Average	6416	244	424	3446	150	776	315	34
	St.dev.	7808	39	327	4286	178	785	235	69
	Median	3942	239	287	1935	97	575	257	10
	Minimum	1680	187	205	799	31	223	123	5
	Maximum	30096	343	1238	16701	697	3417	1158	263
WPS (N = 13)	Average	10424	293	506	5899	264	1328	754	23
	St.dev.	6634	66	275	3617	161	789	353	33
	Median	8401	306	414	4965	206	1143	875	12
	Minimum	4972	187	274	2652	89	514	287	7
	Maximum	30297	372	1316	16973	550	3442	1255	125
I (N = 7)	Average	15133	237	942	7841	297	1566	803	80
	St.dev.	17803	48	516	8732	321	1304	521	115
	Median	6267	236	940	4052	143	1141	755	14
	Minimum	1784	151	332	904	19	243	183	12
	Maximum	47276	299	1659	23771	802	3611	1714	297
BS, WP, WPS, I (N = 74)	Average	10231	266	573	5588	226	1206	589	11
	St.dev.	9248	61	363	4972	195	916	382	61
	Median	7349	257	425	4102	156	840	407	12
	Minimum	1680	130	205	799	19	223	123	5
	Maximum	47276	388	1659	23771	802	3611	1714	297
DH (N = 12)	Average	33324	143	3114	20516	931	4673	1853	456
	St.dev.	35405	76	3408	21382	1020	5078	1914	486
	Median	21761	143	1422	13210	552	2532	953	297
	Minimum	896	42	117	532	21	80	50	5
	Maximum	110457	281	11058	63347	2730	15177	5119	1405

<sup>a</sup>Snow types: fresh snow (FS), diamond dust/surface hoar (DD/SH), blowing snow (FBS), blown snow (BS), wind-packed snow (WP), wind-packed snow at the surface (WPS), snow with ice layers (I), and depth hoar (DH). Also included are the summary statistics of the deposited snow types BS, WP, WPS, and I. N gives the number of samples for each snow type.

temporal trends were detected for most compounds. However, the variability of the concentrations could have masked small trends.

[13] Each snow sample was classified according to the dominant snow type collected (auxiliary material Data Set S1), it is likely that some samples contain multiple snow types. The grains in a given sample represent a collection of thousands of crystals with different origins and post-depositional history that depends on meteorological parameters like temperature and wind and the structure and properties of the snowpack. As a result, the measured concentrations in the same snow type can exhibit a high degree of variability. This is reflected by the results for the DH samples from 4 March indicating that observed concentrations for same or overlapping depths can vary by more than a factor of 10. Average concentrations and further statistical information for all components grouped according to the eight sampled snow types are summarized in Table 2. Like

the composition of the single samples, the average values for the snow types are highly variable. In many cases ranges of concentrations for the snow types are overlapping (Figure 1).

[14] Since Barrow is a coastal location the composition of all samples is dominated by the major sea salt components Cl<sup>-</sup> and Na<sup>+</sup> with average concentrations ranging from <1000 to >33000  $\mu\text{g L}^{-1}$  and <400 to >20000  $\mu\text{g L}^{-1}$ , respectively. The third most abundant component is often Mg<sup>2+</sup>, which originates from sea salt, but also from the Earth's crust. NO<sub>3</sub><sup>-</sup> was also detected in all samples but in most samples at far lower concentrations compared to the sea salt components. The lowest concentrations were normally found for the minor sea salt component Br<sup>-</sup>. The average total ion content was highest in the DH samples followed by I, FBS, and WPS samples. FS and DD/SH samples exhibit on average the lowest total ion content in agreement with previous measurements in the Arctic [Toom-Sauntry and Barrie, 2002; Domine et al., 2004]. Despite

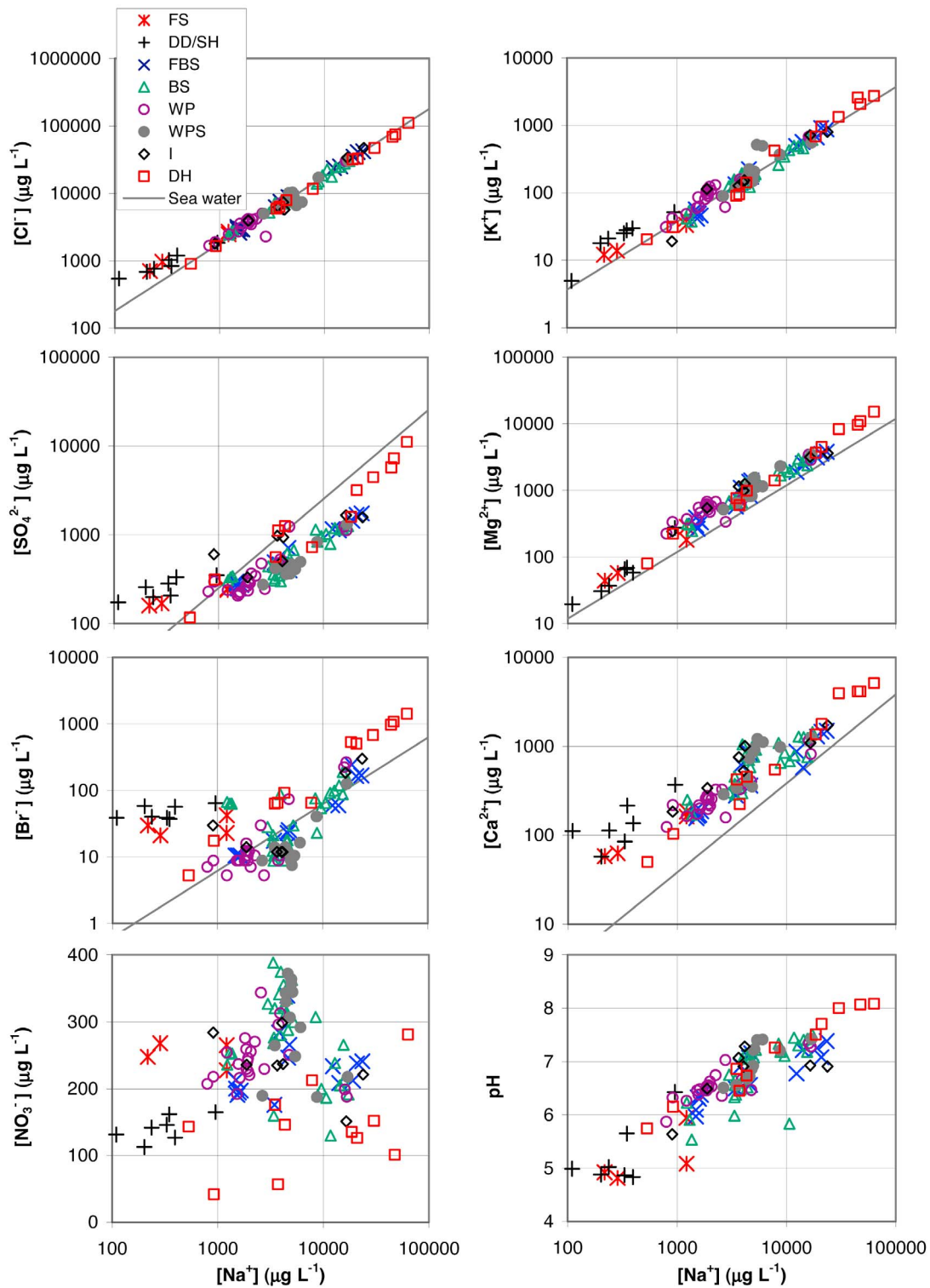


**Figure 1.** (left)  $\text{Cl}^-$ ,  $\text{SO}_4^{2-}$ ,  $\text{Br}^-$ , and  $\text{NO}_3^-$  and (right)  $\text{K}^+$ ,  $\text{Mg}^{2+}$ ,  $\text{Ca}^{2+}$ , and pH versus  $\text{Na}^+$  concentrations determined in all snow samples: fresh snow (FS), diamond dust/surface hoar (DD/SH), blowing snow (FBS), blown snow (BS), wind-packed snow (WP), wind-packed snow at the surface (WPS), snow with ice layers (I), and depth hoar (DH). The lines indicate the standard seawater ratio. The pH was calculated from the estimated alkalinity (see text).

these overall trends, distinct differences can be observed for the different compounds and some different snow types.

## 4. Discussion

### 4.1. Relationships Between Concentrations and Snow Types

[15] The major element concentration (measured as mass per volume of water) in each snow sample can be regarded as a snapshot related to the initial concentration during snow crystal formation and deposition and subsequent physical and chemical processes modifying both the mass of the single impurities and the water volume of the single snow grains during their lifetime. Since the impact of the processes can be different for each individual impurity the relationships between the impurities can vary with the history of the samples. For example, dry and wet deposition can lead to the input of specific impurities [Bergin *et al.*, 1995]. Both processes relate the chemical composition of the snow to the composition of aerosols, which are either directly deposited to the snowpack or incorporated into the snow crystals during the formation process of the snow.

[16] Since Barrow is located near the coast the aerosols in Barrow mainly represent marine sources. As a result, the composition of most of the samples was dominated by sea salt, although the marine aerosols from the sea ice region of the Arctic Ocean can exhibit specific chemical signatures with large amounts of organic compounds and enrichment in  $\text{Ca}^{2+}$  or  $\text{K}^+$  [e.g., Leck and Bigg, 1999; Leck *et al.*, 2002; Frossard *et al.*, 2011]. Moreover, a combination of processes like long-range transport from continental sources, mobilization of dust, and secondary aerosol formation have also been observed at Barrow [e.g., Quinn *et al.*, 2007; Frossard *et al.*, 2011]. Especially in springtime, so-called Arctic Haze, which is comprised mostly of  $\text{SO}_4^{2-}$  aerosols with variable amounts of  $\text{NH}_4^+$ ,  $\text{NO}_3^-$ , dust, organics, and black carbon, can contribute to the total aerosol load in Arctic snow [Barrie and Hoff, 1985; Snyder-Conn *et al.*, 1997; Garbarino *et al.*, 2002; Douglas and Sturm, 2004; Frossard *et al.*, 2011].

[17] At Barrow, wet deposition occurs in the form of snow during the winter season. Three major processes contribute to the accumulation of snow at a given location: Precipitation of fresh snow, precipitation of diamond dust and formation of surface hoar, and remobilization (including vertical transport) of older snow during blowing snow events. The different types of accumulation of snow are represented by the FS, DD/SH, and FBS samples. In the case of FS and DD/SH, the specific mechanisms forming the snow have an important influence [Voisin *et al.*, 2000]. Our DD/SH samples formed under blue sky conditions and their chemical composition was largely controlled by the composition of the ice nucleating particles, possibly modulated by adsorption from the gas phase. In FS samples, riming can introduce compounds such as nitrate, present in the sub-cooled cloud droplets, which are known to be present in clouds down to temperatures of 236 K in the absence of appropriate ice nuclei [Pruppacher and Klett, 1997]. If riming is significant, which depends on the cloud water content, then most of the chemical signature in the snow will be that of cloud droplets, which in turn reflects mainly the composition of the cloud condensation nuclei. The degree of

riming was not determined for our samples, but it will in any case enhance the variability of the composition of the FS samples. Since blowing snow occurs during periods with high wind speeds, the major ion concentrations in these samples are further modified by the effective mobilization, incorporation and deposition of sea salt aerosols due to three different modes of transport. These include creep, saltation, and suspension and they drive the vertical movement of snow grains [e.g., Pomeroy and Goodison, 1997]. After precipitation, the snowpack consists of the snow types BS, WP, WPS, I, and DH. The concentrations of the impurities in these samples reflect the initial composition of the deposited snow plus a subsequent alteration due to deposition or emission related to physical or photochemical processes in the snowpack. The chemical composition of the different snow types we collected was analyzed individually to examine the importance of the physical and chemical processes described above. However, based on the samples available a general discrimination remains impossible for most of the deposited snow types. This is due to the fact that not all snow types could be collected at the same time. However, even with a more comprehensive data set, specific chemical signatures of the single snow types may remain unresolved because different snow types may have similar composition and/or the differences in the composition may be lower than the variability in a given snow type. As a result, the remaining discussion is based on the distinction between the input of new snow due to FS, DD/SH, and FBS and the deposited snow types. In the last case a further distinction of the DH and all further deposited snow types is possible because differences in the composition become obvious (Table 2). Moreover, a paired test using samples of DH and other snow types from 4 and 27 March was performed. A comparison of the concentrations of these specific samples showed that the concentrations in the DH samples were enhanced by a factor of 8 to 11 for all analyzed species except  $\text{NO}_3^-$  compared to the rest of the samples. The  $\text{NO}_3^-$  concentrations in the DH samples were 40% lower. These differences are in general agreement with the differences between the averages of all deposited snow types and the average concentrations in the DH samples (Table 2).

[18] Due to its high concentration in seawater and its low volatility  $\text{Na}^+$  is often used as a conservative tracer for sea salt [e.g., Wagenbach *et al.*, 1998; Rankin *et al.*, 2002; Simpson *et al.*, 2005]. In polar regions, the  $\text{Na}^+$  fraction can be reduced in sea salt aerosols due to the formation of mirabilite in sea ice and frost flowers [Wagenbach *et al.*, 1998; Alvarez-Aviles *et al.*, 2008]. Since the maximum reduction of  $\text{Na}^+$  based on the calculated  $\text{SO}_4^{2-}$  deficit remains below 8% (see below),  $\text{Na}^+$  is here considered without further correction as a reference for the input of sea salt from marine sources (open water in the North Pacific and the Arctic Ocean including different types of sea ice and leads or polynyas) to the snow. Generally,  $\text{Na}^+$  concentrations increased from DD/SH, FS, WP, WPS, BS, I, FBS to DH samples (Table 2).

[19] Concentrations of the main sea salt components ( $\text{Cl}^-$ ,  $\text{Na}^+$ , and  $\text{K}^+$ ) measured in all snow types are presented in Figure 1.  $\text{Cl}^-$  and  $\text{K}^+$  concentrations behave in a similar way compared to  $\text{Na}^+$  in all FBS and deposited snow samples (BS, WP, WPS, I, DH). The ratios between  $\text{Cl}^-$  or  $\text{K}^+$  and  $\text{Na}^+$  are very close to the standard seawater ratio (here and in



all further cases the standard seawater ratios were calculated using the concentrations given by *Millero et al.* [2008]) indicating that  $\text{K}^+$  and  $\text{Cl}^-$  were dominated by marine sources in the majority of the snow types. The FS and DD/SH samples show higher concentrations than expected from the seawater ratio ranging from +10 to +178% for  $\text{Cl}^-$  and +22 to +141% for  $\text{K}^+$ . A similar enrichment in  $\text{Cl}^-$  was also found by *Simpson et al.* [2005] in their samples with low  $\text{Na}^+$  concentrations. A deficit in  $\text{Cl}^-$  was noticeable in 28 samples with the highest deficits in the DH samples. Ten out of 12 DH samples show lower than expected  $\text{Cl}^-$  concentrations (compared to  $\text{Na}^+$ ) with deficits ranging from 0.4 to 14%. The largest absolute  $\text{Cl}^-$  deficit amounts to almost  $9800 \mu\text{g L}^{-1}$ .

[20] While the  $\text{Cl}^-$  and  $\text{K}^+$  enrichments are rather variable in the FS samples, possibly due to varying degrees of riming,  $\text{K}^+$  is strongly enriched in all DD/SH samples. These enrichments are probably related to two different factors. In the case of  $\text{Cl}^-$ , the uptake of chlorine-containing compounds from the gas phase (e.g.,  $\text{HCl}$ ,  $\text{HOCl}$ ) has been found to contribute to elevated  $\text{Cl}^-$  concentrations [*Toom-Sauntry and Barrie*, 2002; *Simpson et al.*, 2005]. In contrast,  $\text{K}^+$  is probably already enriched in the ice nuclei. Ice nucleation on mineral dust is an important process in the formation of ice particles [*Pruppacher and Klett*, 1997]. For example, illite (a clay mineral) contains  $\text{K}^+$  and is a ubiquitous soil mineral that contributes around one third of the soil in the ACP [*Hoose et al.*, 2008].  $\text{K}^+$  is also present in aerosols emitted by biomass burning [e.g., *Andreae and Mettel*, 2001]. In springtime, plumes from biomass burning can easily be transported from Eurasian sources to Barrow and this contributes to the Arctic Haze phenomenon [*Quinn et al.*, 2007; *Frossard et al.*, 2011]. Finally, *Leck and Bigg* [1999] reported cases of strong enrichments of  $\text{K}^+$  in aerosols generated over the Arctic Ocean. All these sources can contribute to the enrichment of  $\text{K}^+$  compared to  $\text{Na}^+$  in the ice nuclei and subsequently in the FS and DD/SH samples [*Domine et al.*, 2011]. Dry deposition of aerosols containing higher  $\text{K}^+$  to  $\text{Na}^+$  ratios could also modify the observed ratios in the deposited snow. However, concentrations in the samples from the snowpack are too high due to the input of sea salt for a detection of dry deposition of non-marine aerosols.

[21] A comparison of the  $\text{SO}_4^{2-}$  and  $\text{Na}^+$  concentrations in all samples (Figure 1) shows a significant correlation for most of the deposited snow types, but with a strong  $\text{SO}_4^{2-}$  deficit compared to the standard seawater ratio of  $\text{SO}_4^{2-}$  to  $\text{Na}^+$ . Only 9 samples of the types BS, WP, I, and DH contained as much or more  $\text{SO}_4^{2-}$  as would be expected compared to seawater. This deficit seems to be introduced with the deposition of blowing snow because all FBS samples were depleted in  $\text{SO}_4^{2-}$ , while the majority of the FS and DD/SH samples were enriched in  $\text{SO}_4^{2-}$ . The DH samples show the highest albeit highly variable  $\text{SO}_4^{2-}$  concentrations with an average of more than  $3000 \mu\text{g L}^{-1}$ , which is, thus, a factor of 5 higher than the average concentration in the rest of the snowpack. The depletion of  $\text{SO}_4^{2-}$  is probably due to the precipitation of mirabilite ( $\text{Na}_2\text{SO}_4 \cdot 10 \text{H}_2\text{O}$ ) at temperatures below  $-8^\circ\text{C}$  [*Wagenbach et al.*, 1998] during the formation of sea ice. This mechanism has previously been invoked to explain  $\text{SO}_4^{2-}$  deficits in frost flowers, aerosols, snow, and ice core samples in the Arctic and Antarctica

[*Rankin et al.*, 2000, 2002; *Kaspari et al.*, 2005; *Alvarez-Aviles et al.*, 2008; *Obbard et al.*, 2009]. The deficits we measured are significant and range between 20 and 75% of the expected  $\text{SO}_4^{2-}$  according to the seawater ratio. The mirabilite formation also impacts the  $\text{Na}^+$  amount in the aerosols. Assuming that all missing  $\text{SO}_4^{2-}$  was removed in the form of mirabilite, we derive a maximum  $\text{Na}^+$  depletion of less than 8%. The enhancement of  $\text{SO}_4^{2-}$  in the DD/SH and FS is similar to  $\text{Cl}^-$  in the same samples and may also be attributed to the presence of  $\text{SO}_4^{2-}$  in the ice nuclei, which is possibly related to non-sea salt  $\text{SO}_4^{2-}$  from Arctic Haze and which is co-deposited during the formation of diamond dust, surface hoar and fresh snow.

[22] In all samples the  $\text{Mg}^{2+}$  to  $\text{Na}^+$  ratio is higher than the standard seawater ratio (Figure 1). The observed lower limit of the  $\text{Mg}^{2+}$  to  $\text{Na}^+$  ratio was close to the seawater ratio of 0.119 [*Millero et al.*, 2008] while the upper limit reached values as high as 0.4. This behavior suggests that both marine and continental sources contributed to the  $\text{Mg}^{2+}$  in the samples and that the continental source is characterized by higher  $\text{Mg}^{2+}$  to  $\text{Na}^+$  ratios compared to seawater. Similar to  $\text{Mg}^{2+}$ ,  $\text{Ca}^{2+}$  is also enriched in all samples compared to seawater (Figure 1) suggesting an additional  $\text{Ca}^{2+}$  input to the snowpack in this region, likely due to dust deposition. The non-sea salt  $\text{Mg}^{2+}$  and  $\text{Ca}^{2+}$  concentrations reached maximum absolute values around 7500 and 2500  $\mu\text{g L}^{-1}$ , respectively. On average, the non-sea salt  $\text{Mg}^{2+}$  and  $\text{Ca}^{2+}$  contributed 44 and 65% to the observed concentrations with maximum contributions on the order of 68 and 96%.

[23] A previous survey of the snow composition in northwestern Alaska indicated that the Brooks Range, which is located approximately 350 km south of Barrow, can be an important source of wind-blown dust for the snowpack [*Douglas and Sturm*, 2004]. The widespread exposure of  $\text{Ca}^{2+}$ -containing rocks in the Brooks Range [e.g., *Newberry et al.*, 1986] may lead to the deposition of  $\text{Ca}^{2+}$  to the snow. Accordingly, snow collected in the Brooks Range contained occasionally even higher  $\text{Ca}^{2+}$  than  $\text{Na}^+$  concentrations [*Douglas and Sturm*, 2004]. The enrichment of  $\text{Ca}^{2+}$  and  $\text{Mg}^{2+}$  in the snow has been observed at other Arctic locations including fresh snow samples in Alert in the Canadian Arctic [*Toom-Sauntry and Barrie*, 2002] and different snow types in Svalbard and Alert [*Domine et al.*, 2004]. Based on 15 years of observations of aerosols at Alert, *Sirois and Barrie* [1999] concluded that on average 82% of the  $\text{Ca}^{2+}$  and 34% of the  $\text{Mg}^{2+}$  in the aerosols originated from soils and the rest originated from sea salt. Therefore, the enrichment of  $\text{Ca}^{2+}$  and  $\text{Mg}^{2+}$  compared to the seawater ratio is not limited to the ACP, but has been encountered over larger regions of the Arctic. This may indicate that long-range transport of aerosols containing  $\text{Ca}^{2+}$  and  $\text{Mg}^{2+}$  contributes to the input of both species to the snowpack at Barrow.

[24] Most of the FS, DD/SH, and DH samples behave differently compared to the rest of the samples. The FS and DD/SH samples are strongly enriched in  $\text{Ca}^{2+}$  and are thus comparable to  $\text{K}^+$ ,  $\text{Cl}^-$ , and  $\text{SO}_4^{2-}$ . On the other hand, the DH samples contain rather constant  $\text{Ca}^{2+}$  to  $\text{Na}^+$  ratios similar to the  $\text{Mg}^{2+}$  content in the same samples.

[25] Previous measurements by *Simpson et al.* [2005] indicated that  $\text{Br}^-$  in the snow is more mobile than  $\text{Na}^+$  leading to a rather homogeneous distribution of  $\text{Br}^-$



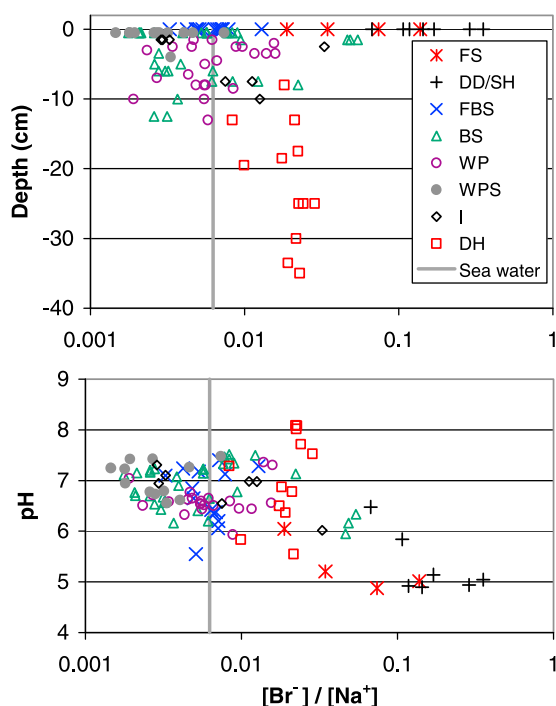


**Figure 2.**  $\text{Br}^-$  to  $\text{Na}^+$  ratio versus (top) depth and estimated (bottom) pH determined in all snow samples: fresh snow (FS), diamond dust/surface hoar (DD/SH), blowing snow (FBS), blown snow (BS), wind-packed snow (WP), wind-packed snow at the surface (WPS), snow with ice layers (I), and depth hoar (DH). The ratios for the FS, DD/SH, and FBS samples are shown at a depth of 0 cm. The vertical line indicates the standard seawater ratio.

compared to  $\text{Na}^+$  in the surface snow between the coast and the Brooks Range. As a result,  $\text{Br}^-$  and  $\text{Na}^+$  were poorly correlated. We identified similar deviations in the  $\text{Br}^-$  to  $\text{Na}^+$  ratio (Figure 1) with strong enrichments or depletions in many samples comparable to the results of *Simpson et al.* [2005]. Only some snow types exhibit consistent deviations from the seawater ratio. For example, the FS and DD/SH samples are always strongly enriched in  $\text{Br}^-$ . Such enrichments are also found in all DH samples. In contrast, most of the WP and almost all of the WPS samples are depleted in  $\text{Br}^-$  compared to  $\text{Na}^+$ . Although sea salt is the major source of  $\text{Br}^-$  to the snowpack, post-depositional physical and chemical processes can modify  $\text{Br}^-$  concentrations.

[26]  $\text{Br}^-$  can be released to the gas phase following photochemical transformation into molecular bromine [*Simpson et al.*, 2007]. Due to its high volatility, molecular bromine is quickly released to the atmosphere where it can participate in chemical processes in the gas phase leading to the catalytic destruction of ozone [e.g., *Simpson et al.*, 2007]. The catalytic cycles are terminated by the formation of hydrobromic acid or other bromine-containing compounds like HOBr,  $\text{Br}_2$ , and  $\text{BrCl}$ , which can subsequently be transferred from the gas phase to the snow [*Toom-Sauntry and Barrie*, 2002]. As a result, the activation of  $\text{Br}^-$  to bromine can lead to a depletion of  $\text{Br}^-$  in the snow while the subsequent deposition of soluble bromine species may lead to an enrichment of  $\text{Br}^-$  compared to the seawater ratio. The highest fraction of

lost  $\text{Br}^-$  in all samples corresponds to 70%, while removal of up to 90% was observed by *Simpson et al.* [2005]. The effect of  $\text{Br}^-$  mobility is shown in Figure 2 indicating the  $\text{Br}^-$  to  $\text{Na}^+$  ratio in all snow samples as a function of the average depth of the sample. At the surface of the snowpack and in the uppermost layers the  $\text{Br}^-$  to  $\text{Na}^+$  ratio is variable ranging from 0.0015 (indicating strong depletion) to 0.35 (indicating strong enhancement). These differences are partly due to different snow types and their formation histories. However, even within the different snow types at the surface the variability remains large.

[27] We estimated alkalinity and pH using the budget of all measured anions and cations and attributing the missing part to either dissolved carbonate or protons. It must be noted that the measured compounds do not represent all acidic and alkaline species present in the snow. Major missing species are ammonium and organic acids. Even at small concentrations their effect and also the analytical uncertainties in the measured species on the calculated alkalinity can be large if the calculated alkalinity becomes small. Due to the estimated presence of carbonate, a very small calculated alkalinity corresponds to a pH of 5.6. Therefore, calculated pH values in the range of 6.2 to 5.0 corresponding to an alkalinity of  $\pm 10 \mu\text{mol L}^{-1}$  must be regarded as highly uncertain. Due to the marine influence, most of the samples showed relatively high alkalinities corresponding to elevated pH values. Only the FS and DD/SH samples showed low estimated pH values. Interestingly, depletion in  $\text{Br}^-$  does not show a relationship with pH (Figure 2). Although *Fickert et al.* [1999] reported an efficient activation of  $\text{Br}^-$  only under acidic conditions, the depletion of  $\text{Br}^-$  was also observed in samples with high estimated pH. In contrast, depletions in  $\text{Br}^-$  are confined to the upper 15 cm of the snowpack (Figure 2). According to the measurements of *France et al.* [2012], at a depth of 15 cm the intensity of the solar radiation in the sampled snowpack typically decreased to a value of  $1/e$ . Therefore, the top 15 cm of the snowpack corresponds to the layer with the most efficient photochemical transformation. In contrast, our samples from deeper layers are always enriched in  $\text{Br}^-$ . This enrichment may be due to a higher input from the still exposed tundra and to the dry deposition of soluble bromine species during the previous fall and winter season, when these layers were exposed at the snow surface. During the dark period an efficient photochemical activation of  $\text{Br}^-$  cannot be expected. Since only DH was sampled in the deeper layers, the metamorphism of the snow may also have influenced  $\text{Br}^-$  concentrations [see below].

[28]  $\text{NO}_3^-$  was detected in all samples (with the exception of one of the DH samples in which  $\text{NO}_3^-$  was below the detection limit). The variability is much smaller than for the major sea salt components (Figure 1). For example, the ratio of the maximum and minimum concentration is less than 10 for  $\text{NO}_3^-$ , while  $\text{Na}^+$  concentrations varied by a factor of more than 550. Accordingly, the ratios between  $\text{NO}_3^-$  and  $\text{Na}^+$  are very variable. The average  $\text{NO}_3^-$  concentrations for the different snow types can be divided in two groups: lower average concentrations in the DD/SH and DH samples around  $140 \mu\text{g L}^{-1}$  and somewhat higher average concentrations between 220 and  $300 \mu\text{g L}^{-1}$  in the other snow types including fresh snow (Table 2). These results indicate

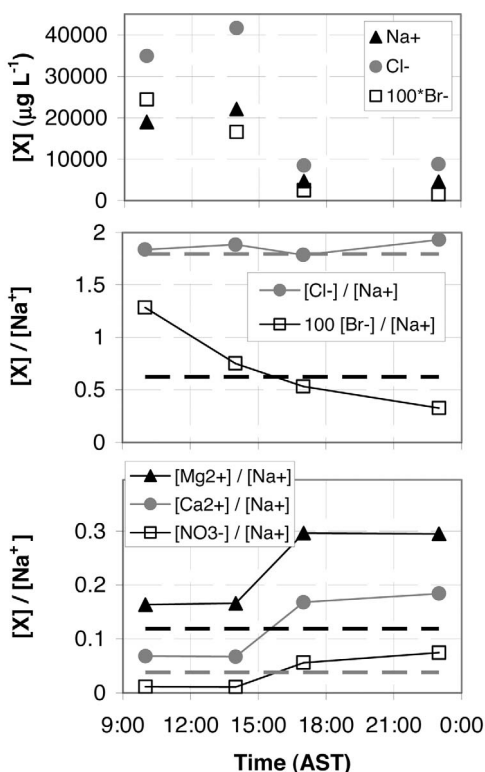


**Figure 3.** Concentrations of (top)  $\text{Na}^+$ ,  $\text{Cl}^-$ , and  $\text{Br}^-$ , (middle) ratios of  $\text{Cl}^-$  and  $\text{Br}^-$  and (bottom)  $\text{Mg}^{2+}$ ,  $\text{Ca}^{2+}$ , and  $\text{NO}_3^-$  to  $\text{Na}^+$  in FBS samples collected on 9 March 2009. The concentrations at 14:00 correspond to the average of two samples collected simultaneously. The dashed horizontal lines correspond to the standard seawater ratios of  $\text{Cl}^-$  (gray),  $\text{Br}^-$  (black),  $\text{Ca}^{2+}$  (gray), and  $\text{Mg}^{2+}$  (black) to  $\text{Na}^+$ .

that sea salt is not the major source of  $\text{NO}_3^-$ . Instead it is mainly incorporated from the gas phase into the snow by scavenging or dry and wet deposition of nitric acid ( $\text{HNO}_3$ ) [Toom-Sauntry and Barrie, 2002].

#### 4.2. Impact of Blowing Snow on the Chemical Composition of the Snowpack

[29] During the OASIS field season, periods with blowing snow were defined by Frieß *et al.* [2011] based on measurements of aerosol optical depth using a MAX-DOAS instrument and visibility using a ceilometer. Blowing snow events were only identified during periods with wind speeds above approximately  $8 \text{ m s}^{-1}$  preventing the formation of DD and SH [Domine *et al.*, 2011]. Therefore, the snow accumulated during blowing snow events can only consist of FBS and FS. At the observed high wind speeds, snow grains travel over the snowpack surface and experience mechanical fracturing, sublimation, and sintering [e.g., Douglas *et al.*, 2008]. The composition of the moving snow crystals is related to the composition of the surface layers of the previously deposited snow and any recent enrichment in these layers can be perpetuated by the blowing snow. Simultaneously, the high wind velocities associated with blowing snow events can lead to aerosol production from local

marine and continental sources impacting the overall composition of the FBS we sampled.

[30] The period from 9 to 11 March 2009 was characterized by an extensive blowing snow event [Frieß *et al.*, 2011]. During this period, the mobilized snow was collected four times on 9 March 2009 as FBS. The time series of the  $\text{Na}^+$ ,  $\text{Cl}^-$ , and  $\text{Br}^-$  concentrations are shown in Figure 3.  $\text{Cl}^-$  and  $\text{Na}^+$  show a slight increase between 9:00 and 14:00 followed by a strong drop in  $\text{Cl}^-$  and  $\text{Na}^+$  concentrations in the late afternoon. Comparable trends for  $\text{Cl}^-$  and  $\text{Na}^+$  species are reflected by the relatively constant ratio close to the standard seawater ratio in all samples (Figure 3). Similarly, constant ratios compared to  $\text{Na}^+$  were observed for  $\text{SO}_4^{2-}$  and  $\text{K}^+$ . While the  $\text{K}^+$  to  $\text{Na}^+$  ratio is very close to the standard seawater ratio  $\text{SO}_4^{2-}$  was always strongly depleted with only one third of the expected  $\text{SO}_4^{2-}$  concentration according to the seawater ratio. The opposite behavior was found for  $\text{Ca}^{2+}$ ,  $\text{Mg}^{2+}$ ,  $\text{NO}_3^-$ , and  $\text{Br}^-$ . Figure 3 demonstrates that  $\text{Ca}^{2+}$  and  $\text{Mg}^{2+}$  were already enriched compared to the seawater ratio in the first two samples with a further strong enrichment in the later two samples. At the same time, the  $\text{NO}_3^-$  to  $\text{Na}^+$  ratio also showed a similar increase between the beginning and the end of the time series.

[31] These significant changes in the chemical composition were accompanied by only small changes in local conditions. For example, the observed wind speed increased slightly from  $15 \text{ m s}^{-1}$  in the morning to  $16 \text{ m s}^{-1}$  in the early afternoon before dropping to values around  $12$  to  $15 \text{ m s}^{-1}$ . During the entire period, the wind speeds were sufficiently high to mobilize the snow. In addition, the observed wind direction turned slightly from easterly in the morning to southeasterly directions in the afternoon. In contrast to the small changes in the local conditions a significant change in the synoptic situation occurred as demonstrated by calculated backward air parcel trajectories for the sampling period (Supplementary Material, Figures 1a–1d). In the morning, air parcels arriving at elevations between 10 and 100 m at Barrow originated from the Central Arctic Ocean and traveled along the northern coast of Canada and Alaska. In the afternoon, the air masses spent longer periods over the estuary of the Mackenzie River before reaching Barrow. Obviously, in the latter case the air masses had sufficient contact with continental snow surfaces and further continental sources to pick up additional  $\text{Ca}^{2+}$  and  $\text{Mg}^{2+}$  while losing a significant part of the initial marine signature. In contrast to  $\text{Cl}^-$ ,  $\text{Br}^-$  shows a constant decrease in concentration as well as in the  $\text{Br}^-$  to  $\text{Na}^+$  ratio (Figure 3). Since  $\text{Br}^-$  shows a general slightly positive correlation with  $\text{Mg}^{2+}$  and  $\text{Ca}^{2+}$  in all snow samples, the  $\text{Br}^-$  decrease cannot be explained by a varying influence from marine to more continental sources. However, the decrease during the daytime hours can be related to an efficient mobilization of  $\text{Br}^-$  due to photochemical processes as discussed above and as proposed by Yang *et al.* [2008] for blowing snow events. This is in excellent agreement with observed  $\text{BrO}$  concentrations on 9 March 2009 rising from below 10 pptV in the morning to maximum concentrations higher than 40 pptV in the afternoon [Frieß *et al.*, 2011].

#### 4.3. Depth Hoar

[32] DH constitutes an important fraction of the total snowpack encountered at Barrow. It is formed when strong

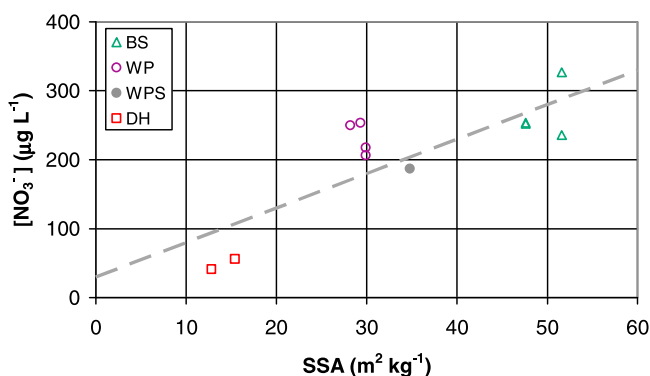


**Figure 4.** Concentration of  $\text{NO}_3^-$  as function of the specific surface area (SSA) of samples collected in the same snow layer: blown snow (BS), wind-packed snow (WP), wind-packed snow at the surface (WPS), and depth hoar (DH).

temperature gradients within the snowpack drive the redistribution of water vapor leading to hexagonal cups as a result of efficient snow metamorphism [Sturm and Benson, 1997]. Major ion concentrations in the DH layers are impacted by several processes. The DH crystals constitute the oldest snow within the snowpack since they are formed from early season snow deposited between October and February. Therefore, the observed concentrations are related to initial snow fall concentrations due to the input by accumulating snow and the subsequent modifications due to dry deposition of aerosols and volatile species from the gas phase. In addition, the early season snow that is metamorphosed into depth hoar has the greatest contact with the tundra surface soil and vegetation surfaces. Finally, the transformation into DH can lead to strong changes in the water volume of the snow grains due to large vertical fluxes of water molecules as a result of the strong vertical temperature gradient in the snowpack [e.g., Colbeck, 1982; Sturm and Benson, 1997]. DH formation can also lead to changes in other snow properties like reductions in density and specific surface area [Domine et al., 2012]. These properties influence the capability of the DH to adsorb and incorporate volatile species. All these process can affect the observed concentrations of impurities in these samples. The encountered major element concentrations are characterized by a larger variability and on average higher concentrations compared to the other snow types. Only  $\text{NO}_3^-$  shows low average DH concentrations comparable to the average  $\text{NO}_3^-$  concentration in DD/SH (Table 1).

[33] Higher major ion concentrations in the springtime snowpack can be caused by higher initial concentrations of the impurities earlier in the season due to more and stronger events of blowing snow and higher production rates of sea salt aerosols leading to higher deposition fluxes of aerosols. A further increase in the concentrations can be due to sublimation during snow metamorphism. Sublimation can mobilize water molecules in the snow crystal while leaving the non-volatile impurities behind. Accordingly, the average concentrations of all species except  $\text{NO}_3^-$  are larger in the DH samples by a factor of 3 to 10 compared to the average concentration of the other deposited snow types. For the two

days (4 and 27 March) with parallel sampling of DH and other snow types these enhancements range between a factor of 8 to 11.

[34] In strong contrast to the other species  $\text{NO}_3^-$  concentrations in the DH samples are even lower than in the other deposited snow types. This is the case for the average of all deposited snow types (Table 2) as well as for the averages of the parallel samples on 4 and 27 March with 40% lower concentrations of  $\text{NO}_3^-$  in the DH. Due to the morphology of DH its specific surface area can be smaller than for most other snow types [Domine et al., 2012]. If  $\text{NO}_3^-$  concentrations in the snow are related to an equilibrium established by adsorption at the surface, lower surface areas can be related to lower  $\text{NO}_3^-$  concentrations. Concomitant measurements of  $\text{NO}_3^-$  and SSA in the same snow layer [Domine et al., 2012] are available for 11 deposited snow samples and are shown in Figure 4. A positive relationship between  $\text{NO}_3^-$  and SSA becomes obvious although the effects of the snow temperature and the atmospheric  $\text{HNO}_3$  concentrations are not included in our calculation. While snow temperatures varied significantly during the field experiments, filter samples of particulate  $\text{NO}_3^-$  including also gas phase  $\text{HNO}_3$  show relatively small variability [Morin et al., 2012]. The linear regression using all 11 deposited snow samples results in the following equation:

$$[\text{NO}_3^-] (\text{in } \mu\text{g L}^{-1}) = (5 \pm 1) \cdot \text{SSA} (\text{in } \text{m}^2 \text{ kg}^{-1}) + (30 \pm 40)$$

Based on these few samples the uncertainty for this relationship remains relatively high expressed by the errors for the slope and the intercept and the coefficient of determination of  $R^2 = 0.67$ . Moreover, the DH samples with parallel SSA measurements showed  $\text{NO}_3^-$  concentrations at the lower end of all observed DH concentrations. The correlation between the SSA and  $\text{NO}_3^-$  in the deposited snow types possibly indicates that for older snow an equilibrium between gas phase  $\text{HNO}_3$  and adsorbed  $\text{NO}_3^-$  (or  $\text{HNO}_3$ ) at the surface of the snow crystals is established making the adsorption the dominating factor. Nevertheless, further factors like the initial  $\text{NO}_3^-$  concentrations in the snow or the solution of  $\text{HNO}_3$  in the solid phase can also contribute to the observed overall  $\text{NO}_3^-$  concentration introducing additional bias in the observations.

[35] Unfortunately, no simultaneous measurements of SSA and  $\text{NO}_3^-$  are available for the FS and DD/SH samples. However, these samples normally exhibit relatively high SSA values well beyond  $60 \text{ m}^2 \text{ kg}^{-1}$  [Domine et al., 2011]. Inserting such values in the above equation results in  $\text{NO}_3^-$  concentrations higher than  $230 \mu\text{g L}^{-1}$  (taking the lower limits of the slope and the intercept). While the range of the observed  $\text{NO}_3^-$  concentrations in the FS sample overlaps with this lower limit, the DD/SH concentrations always remained below  $170 \mu\text{g L}^{-1}$ . This may indicate the formation of DD/SH crystals occurs too rapidly to establish the adsorption equilibrium for  $\text{HNO}_3$ . Due to the formation of diamond dust and surface hoar in the boundary layer or at the snow surface, only  $\text{HNO}_3$  in the boundary layer can be considered as the available gas phase reservoir. If a sufficiently large fraction of gas phase  $\text{HNO}_3$  is adsorbed during the period of the surface hoar or diamond dust formation, the

adsorption can modify the gas phase concentrations and the adsorbed amount of  $\text{HNO}_3$ .

## 5. Conclusions

[36] Snow provides a unique link between the lower atmosphere and the sea ice or winter terrestrial surface. Snow originates in the atmosphere and its initial composition is related to physical and chemical properties of the atmosphere. Once deposited, snow interacts chemically with the lower atmosphere. The focused objective of this study was to determine how depositional and post-depositional processes can affect the chemical composition of snow at an Arctic Coastal location. The vertical and horizontal redistribution of snow and snow chemical compounds leads to a constantly changing chemical equilibrium between the lower atmosphere and snowpack. The snow samples we collected (and the major element concentrations we measured) represent snapshots in time because of the gain or loss of major elements and/or the gain or loss of snow/ice/vapor volume that can all alter the overall concentrations represented by a given sample.

[37] Due to different processes impacting the physical properties of the springtime seasonal snowpack at Barrow, the snowpack exhibits a strong spatial heterogeneity horizontally as well as vertically. A similar heterogeneity is also reflected in the chemical composition of the snowpack. As a result the variability in the snow concentrations is in many cases too high to determine trends in the concentrations as a function of depth or time. However, grouping the samples into unique snow types helps to better distinguish between different stages of the development of the snow. In addition, the snow types we identified represent specific deposition or post-depositional crystal phases. Three types of snow correspond to different forms of the accumulation of new snow while the remaining five snow types represent different steps in the process of metamorphism of deposited snow. Due to the high degree of variability and the limited number of samples, only depth hoar was identified as having a significantly different composition compared to the rest of the deposited snow types. Nevertheless, for a heterogeneous snowpack like what is present at Barrow the snow type remains an important parameter helping to link different stages of snow metamorphism to the chemical composition and should be recorded in future field experiments like density or depth.

[38] The accumulation of the snowpack at Barrow is driven by the deposition of fresh snow, surface hoar, diamond dust and blowing snow. The composition of many of the blowing snow samples was strongly dominated by sea salt and its components. The other snow types contributing to the accumulation exhibited much lower loads of the major sea salt components. This similarity in the chemical composition of the fresh snow, diamond dust and surface hoar is likely related to the similar formation processes of these snow types. Since the composition of the entire snowpack was characterized by sea salt loads much higher than what was found in most of the fresh snow, diamond dust and surface hoar samples, large parts of the accumulated snow probably originated from blowing snow. A further significant source of impurities in the snow was the

deposition of dust as reflected in enhanced  $\text{Mg}^{2+}$  and  $\text{Ca}^{2+}$  concentrations compared to other sea salt components in almost all snow samples. Blowing snow and the entire snowpack showed strong depletions in  $\text{SO}_4^{2-}$  compared to the seawater ratio. Similar to  $\text{Mg}^{2+}$  and  $\text{Ca}^{2+}$ ,  $\text{SO}_4^{2-}$  was also enriched in the FS and DD/SH samples. This probably indicates  $\text{SO}_4^{2-}$  containing aerosols typical for springtime Arctic Haze events were partly removed from the atmosphere by wet deposition. However, this additional  $\text{SO}_4^{2-}$  input to the snowpack was not sufficient to overcome the  $\text{SO}_4^{2-}$  deficit introduced by marine sources. The  $\text{SO}_4^{2-}$  deficit further indicates that the young sea ice surface (and frost flowers that grow on this surface) is prone to the precipitation of mirabilite at temperatures below  $-8^\circ\text{C}$  and this  $\text{SO}_4^{2-}$  depleted source is a major sea salt source for the Barrow snowpack.

[39]  $\text{Br}^-$  showed a more complex behavior than most of the other species due to the different physical and chemical processes impacting  $\text{Br}^-$  concentrations. With marine emissions being the main source of  $\text{Br}^-$  in this region it is mainly introduced into the snowpack with the other sea salt components. However, as result of its ability to undergo chemical transformation into more volatile compounds, it is more mobile after deposition than the other sea salt components. Therefore, a large fraction of the samples were depleted in  $\text{Br}^-$  compared to the standard seawater ratio. This is relevant mainly for samples down to a depth of 15 cm while the few samples from the deeper layers of the snow showed no depletion. However, a reduction of  $\text{Br}^-$  was also observed during a long-lasting blowing snow event. Ultimately, the volatile compounds are transformed back into soluble bromine-containing compounds in the atmosphere, which subsequently undergo dry deposition to the snowpack. As a result, a significant number of samples also show strong  $\text{Br}^-$  enrichments and surface snow samples show a wide spread in  $\text{Br}^-$  concentrations.

[40] Contrary to the sea salt and dust components  $\text{NO}_3^-$  showed a much reduced variability in the concentration in all snow samples.  $\text{NO}_3^-$  is introduced into the snowpack by all three types of new snow. The limited number of samples with concomitant SSA measurements within the snowpack show a positive correlation with the SSA indicating that the  $\text{NO}_3^-$  concentrations in older, deposited snow can be influenced by the adsorption of nitric acid on the snow. Therefore, a large fraction of the  $\text{NO}_3^-$  detected in the deposited snow may readily be available at the surface of the snow grains for chemical transformations leading for example to the formation of nitrogen oxides [Grannas *et al.*, 2007].

[41] Taken in total, the results from this study indicate that changes in sea ice extent, snow precipitation, wind conditions, or vertical temperature gradients can alter the chemical composition of the Arctic coastal snowpack. Climate warming is expected to lead to a diminished Arctic Ocean sea ice extent and to more dynamic sea ice processes. This is expected to lead to more generation of young ice and frost flowers during winter time. The ramifications of these ice driven changes and the expected meteorological response to a warming Arctic are mostly unknown. However, our results suggest that the potentially large predicted changes in sea ice and meteorological conditions in the

Arctic could lead to a different snow chemical regime than is present currently.

[42] **Acknowledgments.** This work is part of the international multi-disciplinary OASIS (Ocean-Atmosphere-Sea Ice-Snowpack) program. It was supported by the French Polar Institute (IPEV) through grant 1017, by the LEFE-CHAT program of INSU-CNRS, and by the U.S. National Science Foundation through grant NSF ATM-0807702. The Barrow Arctic Science Consortium is acknowledged for providing logistical support in the Barrow area.

## References

- Alvarez-Aviles, L., W. R. Simpson, T. A. Douglas, M. Sturm, D. Perovich, and F. Domine (2008), Frost flower chemical composition during growth and its implications for aerosol production and bromine activation, *J. Geophys. Res.*, *113*, D21304, doi:10.1029/2008JD010277.
- Andreae, M. O., and P. Metlet (2001), Emission of trace gases and aerosols from biomass burning, *Global Biogeochem. Cycles*, *15*, 955–966, doi:10.1029/2000GB001382.
- Barrie, L. A., and R. M. Hoff (1985), Five years of air chemistry observations in the Canadian Arctic, *Atmos. Environ.*, *19*, 1995–2010, doi:10.1016/0004-6981(85)90108-8.
- Bergin, M. H., J. L. Jaffrezo, C. I. Davidson, J. E. Dibb, S. N. Pandis, R. Hillamo, W. Maenhaut, H. D. Kuhns, and T. Makela (1995), The contributions of snow, fog and dry deposition to the summer flux of anions and cations at Summit, Greenland, *J. Geophys. Res.*, *100*, 16,275–16,288, doi:10.1029/95JD01267.
- Cho, H., P. B. Shepson, L. A. Barrie, J. P. Cowin, and R. Zaveri (2002), NMR investigation of the quasi-brine layer in ice/brine mixtures, *J. Phys. Chem. B*, *106*, 11,226–11,232, doi:10.1021/jp020449+.
- Colbeck, S. C. (1982), An overview of seasonal snow metamorphism, *Rev. Geophys.*, *20*, 45–61, doi:10.1029/RG020i001p00045.
- Domine, F., R. Sparapani, A. Ianniello, and H. J. Beine (2004), The origin of sea salt in snow on Arctic sea ice and in coastal regions, *Atmos. Chem. Phys.*, *4*, 2259–2271, doi:10.5194/acp-4-2259-2004.
- Domine, F., J.-C. Gallet, M. Barret, S. Houdier, D. Voisin, T. A. Douglas, J. D. Blum, H. J. Beine, C. Anastasio, and F.-M. Bréon (2011), The specific surface area and chemical composition of diamond dust near Barrow, Alaska, *J. Geophys. Res.*, *116*, D00R06, doi:10.1029/2011JD016162.
- Domine, F., J.-C. Gallet, J. Bock, and S. Morin (2012), Structure, specific surface area and thermal conductivity of the snowpack around Barrow, Alaska, *J. Geophys. Res.*, doi:10.1029/2011JD016647, in press.
- Douglas, T. A., and M. Sturm (2004), Arctic haze, mercury and the chemical composition of snow across northwestern Alaska, *Atmos. Environ.*, *38*, 805–820, doi:10.1016/j.atmosenv.2003.10.042.
- Douglas, T. A., M. Sturm, W. R. Simpson, J. D. Blum, L. Alvarez-Aviles, G. J. Keeler, D. K. Perovich, A. Biswas, and K. Johnson (2008), Influence of snow and ice crystal formation and accumulation on mercury deposition to the Arctic, *Environ. Sci. Technol.*, *42*, 1542–1551, doi:10.1021/es070502d.
- Feick, S., K. Kronholm, and J. Schweizer (2007), Field observations on spatial variability of surface hoar at the basin scale, *J. Geophys. Res.*, *112*, F02002, doi:10.1029/2006JF000587.
- Fickert, S., J. W. Adams, and J. N. Crowley (1999), Activation of Br<sub>2</sub> and BrCl via uptake of HOBr onto aqueous salt solutions, *J. Geophys. Res.*, *104*, 23,719–23,727, doi:10.1029/1999JD900359.
- Fierz, C., R. L. Armstrong, Y. Durand, P. Etchevers, E. Greene, D. M. McClung, K. Nishimura, P. K. Satyawali, and S. A. Sokratov (2009), The international classification for seasonal snow on the ground, *IHP-VII Tech. Doc. Hydrol. 83*, UNESCO-IHP, Paris.
- France, J. L., H. J. Reay, M. D. King, D. Voisin, H. W. Jacobi, F. Domine, H. Beine, C. Anastasio, A. MacArthur, and J. Lee-Taylor (2012), Hydroxyl radical and NO<sub>x</sub> production rates, black carbon concentrations and light-absorbing impurities in snow from field measurements of light penetration and nadir reflectivity of on-shore and off-shore coastal Alaskan snow, *J. Geophys. Res.*, doi:10.1029/2011JD016639, in press.
- Frieß, U., H. Sihler, R. Sander, D. Pöhler, S. Yilmaz, and U. Platt (2011), The vertical distribution of BrO and aerosols in the Arctic: Measurements by active and passive differential optical absorption spectroscopy, *J. Geophys. Res.*, *116*, D00R04, doi:10.1029/2011JD015938.
- Frossard, A. A., P. M. Shaw, L. M. Russell, J. H. Kroll, M. R. Canagaratna, D. R. Worsnop, P. K. Quinn, and T. S. Bates (2011), Springtime Arctic haze contributions of submicron organic particles from European and Asian combustion sources, *J. Geophys. Res.*, *116*, D05205, doi:10.1029/2010JD015178.
- Garbarino, J. R., E. Snyder-Conn, T. J. Leiker, and G. L. Hoffman (2002), Contaminants in Arctic snow collected over sea ice, *Water Air Soil Pollut.*, *139*, 183–214, doi:10.1023/A:1015808008298.
- Grannas, A. M., et al. (2007), An overview of snow photochemistry: Evidence, mechanisms and impacts, *Atmos. Chem. Phys.*, *7*, 4329–4373, doi:10.5194/acp-7-4329-2007.
- Hoose, C., U. Lohmann, R. Erdin, and I. Tegen (2008), The global influence of dust mineralogical composition on heterogeneous ice nucleation in mixed-phase clouds, *Environ. Res. Lett.*, *3*, 025003, doi:10.1088/1748-9326/3/2/025003.
- Jaffrezo, J. L., N. Calas, and M. Bouchet (1998), Carboxylic acids measurements with ionic chromatography, *Atmos. Environ.*, *32*, 2705–2708, doi:10.1016/S1352-2310(98)00026-0.
- Kaspari, S., D. A. Dixon, S. B. Sneed, and M. J. Handley (2005), Sources and transport pathways of marine aerosol species into West Antarctica, *Ann. Glaciol.*, *41*, 1–9, doi:10.3189/172756405781813221.
- Kuo, M. H., S. G. Moussa, and V. F. McNeill (2011), Liquid-like layers on ice in the environment: Bridging the quasi-liquid and brine layer paradigms, *Atmos. Chem. Phys. Discuss.*, *11*, 8145–8172, doi:10.5194/acpd-11-8145-2011.
- Leck, C., and E. K. Bigg (1999), Aerosol production over remote marine areas—A new route, *Geophys. Res. Lett.*, *26*, 3577–3580, doi:10.1029/1999GL010807.
- Leck, C., M. Norman, E. K. Bigg, and R. Hillamo (2002), Chemical composition and sources of the high Arctic aerosol relevant for cloud formation, *J. Geophys. Res.*, *107*(D12), 4135, doi:10.1029/2001JD001463.
- Lemke, P., et al. (2007), Observations: Changes in snow, ice and frozen ground, in *Climate Change 2007: The Physical Science Basis. Contribution of Working Group I to the Fourth Assessment Report of the Intergovernmental Panel on Climate Change*, pp. 339–383, Cambridge Univ. Press, Cambridge, U. K.
- Millero, F. J., R. Feistel, D. G. Wright, and T. J. McDougall (2008), The composition of standard seawater and the definition of the reference-composition salinity scale, *Deep Sea Res., Part 1*, *55*, 50–72, doi:10.1016/j.dsr.2007.10.001.
- Morin, S., J. Erbland, J. Savarino, F. Dominé, J. Bock, U. Frieß, H. W. Jacobi, H. Sihler, and J. M. F. Martins (2012), An isotopic view on the connection between photolytic emissions of NO<sub>x</sub> from the Arctic snowpack and its oxidation by reactive halogens, *J. Geophys. Res.*, *117*, D00R08, doi:10.1029/2011JD016618.
- Newberry, R. J., J. T. Dillon, and D. D. Adams (1986), Regionally metamorphosed, calc-silicate-hosted deposits of the Brooks Range, northern Alaska, *Econ. Geol.*, *81*, 1728–1752, doi:10.2113/gsecongeo.81.7.1728.
- Obbard, R. W., H. K. Roscoe, E. W. Wolff, and H. M. Atkinson (2009), Frost flower surface area and chemistry as a function of salinity and temperature, *J. Geophys. Res.*, *114*, D20305, doi:10.1029/2009JD012481.
- Pomeroy, J. W., and B. E. Goodison (1997), Winter and snow, in *The Surface Climates of Canada*, edited by W. G. Bailey, T. R. Oke, and W. R. Rouse, pp. 68–100, McGill-Queen's Univ. Press, Montreal, Que., Canada.
- Pruppacher, H. R., and J. D. Klett (1997), *Microphysics of Clouds and Precipitation*, Kluwer, Dordrecht, Netherlands.
- Quinn, P. K., G. Shaw, E. Andrews, E. G. Dutton, T. Ruoho-Airola, and S. L. Gong (2007), Arctic haze: Current trends and knowledge gaps, *Tellus, Ser. B*, *59*, 99–114, doi:10.1111/j.1600-0889.2006.00238.x.
- Rankin, A. M., V. Auld, and E. W. Wolff (2000), Frost flowers as a source of fractionated sea salt aerosol in the polar regions, *Geophys. Res. Lett.*, *27*, 3469–3472, doi:10.1029/2000GL011771.
- Rankin, A. M., E. W. Wolff, and S. Martin (2002), Frost flowers: Implications for tropospheric chemistry and ice core interpretation, *J. Geophys. Res.*, *107*(D23), 4683, doi:10.1029/2002JD002492.
- Ricard, V., J. L. Jaffrezo, V. Kerminen, R. E. J. Hillamo, M. Sillanpää, S. Ruellan, C. Liousse, and H. Cachier (2002), Two years of continuous aerosol measurements in northern Finland, *J. Geophys. Res.*, *107*(D11), 4129, doi:10.1029/2001JD000952.
- Simpson, W. R., L. Alvarez-Aviles, T. A. Douglas, M. Sturm, and F. Dominé (2005), Halogens in the coastal snow pack near Barrow, Alaska: Evidence for active bromine air-snow chemistry during springtime, *Geophys. Res. Lett.*, *32*, L04811, doi:10.1029/2004GL021748.
- Simpson, W. R., et al. (2007), Halogens and their role in polar boundary-layer ozone depletion, *Atmos. Chem. Phys.*, *7*, 4375–4418, doi:10.5194/acp-7-4375-2007.
- Sirois, A., and L. A. Barrie (1999), Arctic lower tropospheric aerosol trends and composition at Alert, Canada: 1980–1995, *J. Geophys. Res.*, *104*, 11,599–11,618, doi:10.1029/1999JD900077.
- Snyder-Conn, E., J. R. Garbarino, G. L. Hoffman, and A. Oelkers (1997), Soluble trace elements and total mercury in Arctic Alaskan snow, *Arctic*, *50*, 201–215.
- Sturm, M., and C. S. Benson (1997), Vapor transport, grain growth and depth-hoar development in the subarctic snow, *J. Glaciol.*, *43*, 42–59.
- Sturm, M., and G. E. Liston (2003), The snow cover on lakes of the Arctic Coastal Plain of Alaska, U.S.A., *J. Glaciol.*, *49*, 370–380, doi:10.3189/172756503781830539.

- Toom-Saunty, D., and L. A. Barrie (2002), Chemical composition of snow-fall in the high Arctic: 1990–1994, *Atmos. Environ.*, *36*, 2683–2693, doi:10.1016/S1352-2310(02)00115-2.
- Voisin, D., M. Legrand, and N. Chaumerliac (2000), Scavenging of acidic gases (HCOOH, CH<sub>3</sub>COOH, HNO<sub>3</sub>, HCl, and SO<sub>2</sub>) and ammonia in mixed liquid-solid water clouds at the Puy de Dôme mountain (France), *J. Geophys. Res.*, *105*, 6817–6835, doi:10.1029/1999JD900983.
- Wagenbach, D., F. Ducroz, R. Mulvaney, L. Keck, A. Minikin, M. Legrand, J. S. Hall, and E. W. Wolff (1998), Sea-salt aerosol in coastal Antarctic regions, *J. Geophys. Res.*, *103*, 10,961–10,974, doi:10.1029/97JD01804.
- Wettlaufer, J. S. (1999), Impurity effects in the premelting of ice, *Phys. Rev. Lett.*, *82*, 2516–2519, doi:10.1103/PhysRevLett.82.2516.
- Yang, X., J. A. Pyle, and R. A. Cox (2008), Sea salt production and bromine release: Role of snow on sea ice, *Geophys. Res. Lett.*, *35*, L16815, doi:10.1029/2008GL034536.

---

J. Cozic, H. W. Jacobi, J. L. Jaffrezo, and D. Voisin, Laboratoire de Glaciologie et Géophysique de l'Environnement, CNRS/Université Joseph Fourier – Grenoble 1, UMR 5183, 54, rue Molière, Saint Martin d'Hères F-38402, France. (jacobi@lgge.obs.ujf-grenoble.fr)

T. A. Douglas, Environmental Sciences, U.S. Army Cold Regions Research and Engineering Laboratory, PO Box 35170, Bldg. 4070, Fort Wainwright, AK 99703-0170, USA.